

To Compute or not to Compute? Adaptive Smart Sensing in Resource-Constrained Edge Computing

Luca Ballotta¹, Graduate Student Member, IEEE, Giovanni Peserico²,
 Francesco Zanini³, Graduate Student Member, IEEE, and Paolo Dini⁴

Abstract—We consider a network of smart sensors for edge computing application that sample a signal of interest and send updates to a base station for remote global monitoring. Sensors are equipped with sensing and compute, and can either send raw data or process them on-board before transmission. Limited hardware resources at the edge generate a fundamental *latency-accuracy trade-off*: raw measurements are inaccurate but timely, whereas accurate processed updates are available after *computational delay*. Also, if sensor on-board processing entails data compression, latency caused by wireless communication might be higher for raw measurements. Hence, one needs to decide when sensors should transmit raw measurements or rely on local processing to maximize overall network performance. To tackle this sensing design problem, we model an estimation-theoretic optimization framework that embeds computation and communication delays, and propose a Reinforcement Learning-based approach to dynamically allocate computational resources at each sensor. Effectiveness of our proposed approach is validated through numerical simulations with case studies motivated by the Internet of Drones and self-driving vehicles.

Index Terms—Communication latency, computation latency, edge computing, Q-learning, resource allocation, sensing design.

I. INTRODUCTION

Distributed computation scenarios such as the Internet of Things and Industry 4.0 represent a major breakthrough in engineering applications, whereby coordination and cooperation of sensing and actuation moves away from classical centralized controllers to servers and devices at the network edge. This empowers multiple local systems to achieve together complex goals at global level: this happens with management of electricity and energy harvesting in smart grids [1], [2], efficient resource utilization in smart agriculture [3], [4], modularization and productivity enhancement in Industry 4.0 [5], [6], [7], and urban traffic eased by interconnected vehicles [8], [9].

In particular, recent advances in both embedded electronics, with powerful micro controllers and GPU processors [10],

This work has been partially funded by the Italian Ministry of Education, University and Research (MIUR) through the PRIN project no. 2017NS9FEY entitled “Realtime Control of 5G Wireless Networks: Taming the Complexity of Future Transmission and Computation Challenges” and through the initiative “Departments of Excellence” (Law 232/2016). The views and opinions expressed in this work are those of the authors and do not necessarily reflect those of the funding institutions.

Luca Ballotta, Giovanni Peserico, and Francesco Zanini are with the Department of Information Engineering, University of Padova, 35131 Padova, Italy (e-mail: {luca.ballotta.1; giovanni.peserico; francesco.zanini.3}@phd.unipd.it).

Giovanni Peserico is also with Autec s.r.l., 36030 Caldogno, Italy.

Paolo Dini is with the Centre Tecnologic de Telecomunicacions de Catalunya (CTTC/CERCA), 08860 Barcelona, Spain (e-mail: paolo.dini@cttc.es).

The first three authors contributed equally to this work.

[11], and new-generation communication protocols for massive networks, such as 5G [12], [13], are currently pushing network systems to rely on sensors and, more in general, edge devices to carry most of the computational burden. Indeed, distributed computation paradigms such as edge and fog computing [14], [15], [16], [17] and federated and decentralized learning [18], [19], [20], even though still in their infancy, enjoy febrile activity and excitement across the research community.

Despite the growing amount of resources and technological development, emerging edge technologies are still limited compared to powerful centralized servers and cloud. Indeed, resource-constrained devices still severely trade several factors, such as hardware cost, processing speed, and energy consumption. In particular, the benefits of refining data on-board smart sensors come at the cost of non-negligible processing time.

We consider a group of edge smart sensors, such as compute-equipped IoT nodes or aerial vehicles, that measure a signal of interest – e.g., voltage in a smart grid, or movements of vehicles for surveillance – and transmit sensory data to a common base station that performs remote global monitoring and possibly decision-making. Limited hardware resources induce a *latency-accuracy trade-off* at each sensor, that can supply either raw, inaccurate samples of the monitored signal, or locally refine data to transmit more precise information at the cost of *processing delay* caused by constrained computation. Local processing may consist of averaging or filtering of noisy samples, or compression of images or other high-dimensional data [21], [22], to mention a few examples. Because the monitored system evolves dynamically, delays in transmitted measurements may hinder their usefulness in real-time tasks, so that sensing design for multiple, heterogeneous sensors becomes challenging. In particular, as these cooperate, it is unclear which of them should rely on local computation to transmit accurate information, and which ones would be better off sending raw data. Also, wireless channel constraints such as limited bandwidth introduce non-negligible *communication latency*, further increasing complexity of the sensing design. Specifically, local processing might compress acquired samples, so that transmission of raw data to the base station takes longer.

A. Related literature

Resource allocation in terms of sensor and actuator selection represents a major research topic in IT, robotics, and control. Classically, the need for selection emerges from maximization of a performance metric subject to limited resource budget, being it of economical, functional (e.g., weight of autonomous

platforms), spatial (*e.g.*, locations to place sensors), or other nature. Typical works in this field [23], [24], [25], [26], [27], [28], [29], [30], [31] focus on such budget-related constraints and pay little attention to impact on system dynamics. For example, [23] proposes selection strategies based on coverage probability and energy consumption for a target tracking problem, [31] studies a clustering-based selection to address communication constraints in underwater environments, and [29] tackles placement of cheap and expensive sensors to optimize reconstruction of dynamical variables. The aforementioned works, even though possibly addressing computation and/or communication issues, either care about energy consumption or address latency in a qualitative way, but do not use that information to compute an exact performance metric that depends on the system dynamics. Another, more control theoretic, body of work exploits tools from set-valued optimization, *e.g.*, submodular functions with matroid constraints [32], or studies analytical bounds [33] or convex formulations [34], [28], yet within a static framework that does not address changes in the overall dynamics.

In a similar realm, control theory is traditionally concerned with either channel-aware estimation and control, or co-design of communication and controller, addressing wireless channel issues such as unreliability, latency, and more in general limited information [35], [36], [37], [38], [39], [40], [41]. For example, [35], [41] are concerned with rate-constrained stabilizability, while [36], [40] address LQR and LQG optimal control. More recently, performance of wireless cyber-physical systems subject to state and input constraints has been thoroughly investigated leveraging model-based prediction and optimization tools such as MPC [42], [43], [44], [45]. However, also this line of work does not consider processing-dependent delays and their effect on dynamics and performance. Even in recent works on co-design of sensing, communication, and control [46], [47], [48] there is still no unifying framework that quantitatively relates sensing and data processing on resource-limited platforms to performance of estimation and control in dynamical networked systems.

Finally, a recent body of literature tailored to edge and fog computing studies distributed computation on-board resource-constrained devices, focusing on minimization of delays [49], [50], [51], [52] or latency-dependent energy consumption [53]. While there is a clear, empirically supported intuition that outdated sensory information is detrimental to performance because of the dynamical nature of monitored system, the above line of work does not tackle exact performance metrics (which may be too complicated to be computed or unknown), but employs delay or (functions of) Age of Information [54], [55] as heuristic proxies to the true cost function. Also, most works, *e.g.*, [48], assume that sensors measure decoupled processes, thus greatly reducing complexity of the network design, but also applicability to control or robotic applications.

B. Novel Contribution and Paper Organization

In contrast to previous work, we aim to jointly address sensor local processing, computation and communication latency, and system dynamics within an optimal sensing design.

In [56], the authors proposed a general model for a processing network, including impact of computation-dependent

delays on system dynamics, and provided a heuristic sensing design. A major limitation is that the designed policy is static, *i.e.*, sensors are configured at the beginning and cannot adapt to the monitored signal during operations, which may hinder performance. For example, time-varying or nonlinear system dynamics generally prevents the optimal sensing or control design to be static (or even stationary). Also, it was assumed that sensors could use an unlimited buffer to store new samples while processing a measurement. We circumvent such issues through a novel optimization framework that builds on the insight presented in [56]. Moreover, this paper considerably expands the preliminary version [57] as described next.

First, we propose a new model for a *processing network*, which tailors more realistic sampling by resource-constrained smart sensors (Section II). The latter can adapt their local computation and exploit the latency-accuracy trade-off online to maximize global network performance, by choosing to either transmit raw samples or locally refine data through some on-board algorithms. In addition, motivated by the performance-driven selection addressed in [56], we let sensors (temporary) stand by in order to alleviate the computational burden at the base station. Roughly speaking, this helps because data fusion may degrade the monitoring quality if the amount of sensory data transmitted to the base station overwhelms the latter's computational resources. Further, this design feature has the remarkable side effect of saving energy consumption while at the same time improving global performance.

In Section II-B, we formulate a sensing design problem to manage computation resources in a network of heterogeneous sensors within an optimization framework. This is done by exactly computing an estimation-theoretic performance metric with dynamical parameters and computational delays. To partially overcome intractability of the problem, we formulate a simplified version in Section III, and tackle it via a Reinforcement Learning approach that is detailed in Section IV. Reinforcement Learning, and data-driven methods in general, are now popular in network systems and edge computing because of challenges of real-world scenarios [58], [59], [60].

Finally, in Section V we validate our proposed approach through two simulations motivated by heterogeneous smart sensing for autonomous driving and an Internet-of-Drones tracking scenario, showing that accounting for processing latency can improve performance through careful allocation of computational resources. In particular, we address realistic wireless communication by leveraging an industrial-oriented discrete-event simulator (OMNeT++) that accurately models electromagnetic field and lower layers of the protocol stack.

II. SETUP AND PROBLEM FORMULATION

In this section, we first model a processing network composed of smart sensors (Section II-A), and then formulate the sensing design as an optimal estimation problem (Section II-B).

A. System model

Dynamical System. The signal of interest is described by a time-varying discrete-time linear dynamical system,

$$x_{k+1} = A_k x_k + w_k, \quad (1)$$

where $x_k \in \mathbb{R}^n$ collects the to-be-estimated variables (state) of the system, $A_k \in \mathbb{R}^{n \times n}$ is the state matrix, and white noise $w_k \sim \mathcal{N}(0, W_k)$ captures model uncertainty. Such class of models is widely used in control applications, by virtue of their simplicity but also powerful expressiveness [61], [62], [63], [64], [26]. For example, a standard approach in control of dynamical systems modeled through nonlinear differential equations is to approximate the original model as a parameter- or time-varying linear system, for which efficient control and optimization techniques are known [26], [65], [66].

In view of wireless transmission of sensor samples, we assume discrete-time dynamics with time step T , where subscript $k \in \mathbb{N}$ means the k th time instant kT . Without loss of generality, we fix the first instant $k_0 = 1$. The sampling time T represents a suitable time scale for the global monitoring and, possibly, decision-making task at hand. For example, typical values of T are one or two seconds for trajectory planning of ground robots, while higher frequency is required for drones performing a fast pursuit or self-driving applications.

Smart Sensors. The system modeled by (1) is measured by N smart sensors (or simply sensors) gathered in the set $\mathcal{V} = \{1, \dots, N\}$, which output a noisy version of the state x_k ,

$$y_k^{(i)} = x_k + v_k^{(i)}, \quad v_k^{(i)} \sim \mathcal{N}(0, V_{i,k}), \quad (2)$$

where $y_k^{(i)}$ is the measurement collected by the i th sensor at time k , for any $i \in \mathcal{V}$, and $v_k^{(i)}$ is measurement noise.

Sensors can either communicate raw measurements or process the latter locally before transmission. Such processing may consist of compression or filtering of raw data, or of more complex tasks such as feature extraction from visual data or 3D point clouds. Sensors face a *latency-accuracy trade-off* through limited computation: raw measurements are less accurate, but local data processing introduces extra computational delay. In particular, uncertainty about the true dynamics, modeled in (1) through the noise term w_k , progressively makes outdated measurements less informative about the current state of the system, so that high accuracy alone might not pay off in real-time monitoring.

For example, consider a car that is approximately moving at constant speed, where w_k captures unmodeled movements such as small accelerations: as time goes by, knowledge of the current position of the car through its nominal model (constant speed) becomes more and more imprecise because of unknown terms hidden by w_k (accelerations), which progressively deviate the car from its nominal trajectory. In this case, a sensor may prefer to sample the system (*e.g.*, capture images of the car) more often, rather than spending time to obtain precise, but outdated, position measurements.

We formalize the latency-accuracy trade-off as follows.

Assumption 1 (Sensing modes). Each sensor $i \in \mathcal{V}$ can be in *raw*, *processing*, or *sleep* mode.

Raw mode: measurements are generated after delay $\tau_{i,\text{raw}}$ with noise covariance $V_{i,k} \equiv V_{i,\text{raw}}$.

Processing mode: measurements are generated after *processing* delay $\tau_{i,\text{proc}}$ with noise covariance $V_{i,k} \equiv V_{i,\text{proc}}$.

Sleep mode: the sensor is temporary set idle (*asleep*): neither data sampling nor transmission occur under this mode.

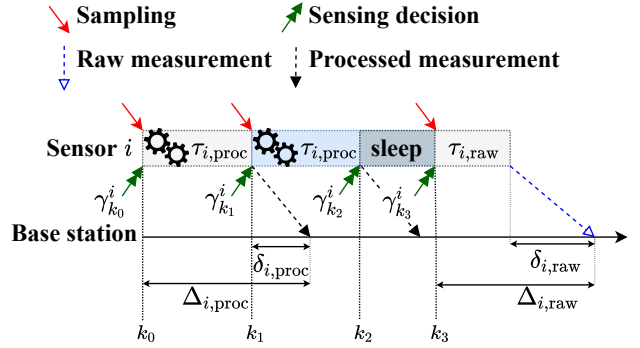


Fig. 1. **Data collection and transmission.** Computation at the i th sensor is ruled by sensing policy π_i . Here, sensing decisions $\{\gamma_{k_j}^i\}_{j=0}^3 = \{p, p, s, r\}$ are shown and (4) reads $\mathcal{K}_i[0] = s_i^0(k_0) = k_0$, $\mathcal{K}_i[1] = s_i(k_0) = k_1$, and $\mathcal{K}_i[2] = s_i(k_1) = k_3$. Measurements are received after delays induced by local computation (rectangular blocks) and communication (dashed arrows). For example, under $\gamma_{k_0}^i = p$, the sample acquired at time k_0 is first processed (with processing delay $\tau_{i,\text{proc}}$), then transmitted at time $k_1 = k_0 + \tau_{i,\text{proc}}$ (with communication delay $\delta_{i,\text{proc}}$), and finally received at the base station at time $k_1 + \delta_{i,\text{proc}} = k_0 + \Delta_{i,\text{proc}}$ (with delay at reception $\Delta_{i,\text{proc}}$).

Assumption 2 (Latency-accuracy trade-off). For each sensor $i \in \mathcal{V}$, it holds $\tau_{i,\text{proc}} > \tau_{i,\text{raw}}$ and $V_{i,\text{raw}} \succ V_{i,\text{proc}}$.¹

Similarly to [56], Assumption 2 models high accuracy as long computation (Fig. 1) and "small" covariance (intensity) of measurement noise, *e.g.*, raw distance measurements may have uncertainty of 1m^2 while processed ones of 0.1m^2 .

Next, we define how local operations are ruled overtime.

Definition 1 (Sensing policy). A *sensing policy* for the i th sensor is a sequence of categorical decisions $\pi_i \doteq \{\gamma_k^i\}_{k \geq k_0}$. If $\gamma_k^i = r$, measurement $y_k^{(i)}$ is transmitted raw; if $\gamma_k^i = p$, $y_k^{(i)}$ is processed; if $\gamma_k^i = s$, no measurement is acquired at time k .

According to Definition 1, different sensing modes can be alternated online. However, because of constrained resources, a sensor cannot acquire measurements arbitrarily often. The actual sampling frequency is determined as formalized next.

Assumption 3 (Sampling frequency). Assume that the i th sensor acquires a sample at time k under either raw ($\gamma_k^i = r$) or processing ($\gamma_k^i = p$) mode. Let time k' be defined as

$$k' \doteq \begin{cases} k + \tau_{i,\text{raw}} & \text{if } \gamma_k^i = r \\ k + \tau_{i,\text{proc}} & \text{if } \gamma_k^i = p \end{cases}. \quad (3a)$$

Then, the next sample (under any mode) occurs at time $s_i(k)$,

$$s_i(k) \doteq \min_{h \in \mathbb{N}} \{h \geq k' : \gamma_h^i \neq s\}. \quad (3b)$$

Finally, the sequence of all sampling instants \mathcal{K}_i is given by

$$\mathcal{K}_i = \{s_i^l(k_0)\}_{l \geq 0}, \quad (4a)$$

¹Covariance matrices are ordered according to Löwner order of positive semidefinite matrices. Even though this is a partial order, we require it in our model to express the latency-accuracy trade-off unambiguously.

where consecutive sampling times are defined by the recursion

$$\begin{aligned} s_i^{l+1}(k) &= s_i(s_i^l(k)) \\ s_i^0(k_0) &\doteq \min_{h \in \mathbb{N}} \{h \geq k_0 : \gamma_h^i \neq s\}, \end{aligned} \quad (4b)$$

and $\mathcal{K}_i[l]$ denotes the l th element of the sequence, with $l \in \mathbb{N}$.

In words, Assumption 3 states that sensors can acquire a new sample only after the previous measurement has been transmitted. This is a realistic assumption if agents have limited storage resources [67]. The effect of a sensing policy on sampling and local data processing is illustrated in Fig. 1.

Remark 1 (Multiple processing modes). Smart sensors may have multiple options to process data. For example, camera-equipped robots might choose among several geometric inference algorithms for perception (or instances of anytime algorithms [68]) to trade latency for accuracy. While we stick to a single processing mode for the sake of simplicity and exposition, our framework can also be extended in that respect.

Wireless channel. All sensors transmit data to a common base station through a shared wireless channel. The latter induces *communication latency* that may further delay transmitted updates. We let $\delta_{i,\text{raw}}$ and $\delta_{i,\text{proc}}$ denote communication delays of raw and processed data transmitted by the i th sensor, respectively. In general, $\delta_{i,\text{raw}}$ and $\delta_{i,\text{proc}}$ might be different, depending on possible compression performed by data processing. In case $\delta_{i,\text{raw}} = \delta_{i,\text{proc}}$, we denote both communication delays by δ_i . Finally, the total delay experienced by transmitted data from sampling to reception at the base station (*delay at reception*) is given by $\Delta_{i,\text{raw}} = \tau_{i,\text{raw}} + \delta_{i,\text{raw}}$ for raw and $\Delta_{i,\text{proc}} = \tau_{i,\text{proc}} + \delta_{i,\text{proc}}$ for processed data. Data sampling, processing, and transmission are depicted in Fig. 1.

Base Station. Data are transmitted to a base station in charge of estimating the state of the system x_k in real time. Such estimation enables remote global monitoring and decision-making, *e.g.*, coordinated trajectory tracking or exploration. Let \hat{x}_k denote the real-time estimate of x_k . In view of the sequential nature of centralized data processing, when limited computational resources are available at the base station, the real-time estimate of x_k is computed in ϕ_k time (*fusion delay*), needed to process sensory data used in the update [56]. For example, consider Fig. 2: from time k_1 through k_4 , new data are received at the base station (green dashed arrows). If the estimation routine starts at time k_4 , it will take ϕ_{k_5} to process all newly received sensory data (possibly, also old ones if some data arrive out of sequence), and hence the next updated state estimate, \hat{x}_{k_5} , will be available at time $k_5 = k_4 + \phi_{k_5}$. Hence, fusion delays induce open-loop predictions that degrade quality of the computed estimates (similarly to what discussed about local sensor processing), and motivate sleep mode to reduce the incoming stream of sensory data and improve overall performance [56].

Assumption 4 (Available sensory data). In view of Assumptions 1, 3, all sensory data available at the base station and

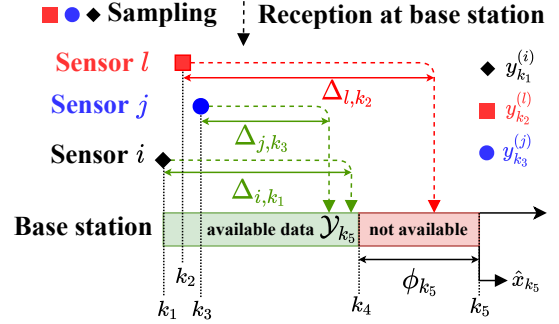


Fig. 2. **Data processing at the base station.** Resource-constrained centralized processing introduces *fusion delay* ϕ_{k_5} to estimate x_{k_5} . Measurements $y_{k_1}^{(i)}$ and $y_{k_3}^{(j)}$ are received before computation starts at time $k_4 = k_5 - \phi_{k_5}$ and are used to compute \hat{x}_{k_5} , *i.e.*, $y_{k_1}^{(i)}, y_{k_3}^{(j)} \in \mathcal{Y}_{k_5}$, while $y_{k_2}^{(l)}$ is received after time k_4 and cannot be used in estimation of x_{k_5} , *i.e.*, $y_{k_2}^{(l)} \notin \mathcal{Y}_{k_5}$.

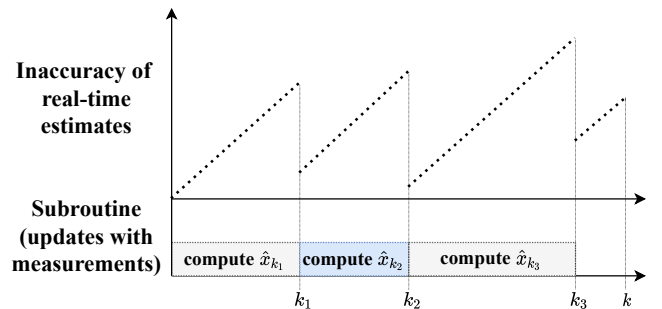


Fig. 3. **Real-time estimation at the base station.** The state estimate is updated at each point in time (top). Because of limited resources at the base station, open-loop updates are performed whenever fresh sensory data are being processed (bottom), causing estimation to degrade overtime through additive noise w_k in nominal dynamics (1). As soon as the data processing subroutine produces an updated estimate with new measurements, *e.g.*, \hat{x}_{k_1} at time k_1 , the estimation inaccuracy is reduced. Note that the top plot is qualitative: the estimate quality does not degrade linearly, in general.

used to compute \hat{x}_k at time k are

$$\begin{aligned} \mathcal{Y}_k &\doteq \bigcup_{i \in \mathcal{V}} \bigcup_{l \in \mathbb{N}} \left\{ \left(y_{\mathcal{K}_i[l]}^{(i)}, V_{i,\mathcal{K}_i[l]} \right) : \mathcal{K}_i[l] + \Delta_{i,\mathcal{K}_i[l]} + \phi_k \leq k \right\} \\ \Delta_{i,\mathcal{K}_i[l]} &\doteq \begin{cases} \Delta_{i,\text{raw}} & \text{if } \gamma_{\mathcal{K}_i[l]}^i = r \\ \Delta_{i,\text{proc}} & \text{if } \gamma_{\mathcal{K}_i[l]}^i = p \end{cases}, \end{aligned} \quad (5)$$

where the l th measurement from the i th sensor $y_{\mathcal{K}_i[l]}^{(i)}$ is sampled at time $\mathcal{K}_i[l]$ and received after overall delay $\Delta_{i,\mathcal{K}_i[l]}$, and ϕ_k is the time needed to compute \hat{x}_k at the base station.

According to Assumption 4, a measurement $y_h^{(i)}$ can be used to compute the estimate of x_k in real time if it is successfully delivered to the base station (with delay at reception $\Delta_{i,h}$) before or at time $k - \phi_k$, where ϕ_k is the amount of time needed to compute \hat{x}_k . Data processing at the base station with limited resources and data availability is depicted in Fig. 2.

Remark 2 (Real-time estimation). Based on the above discussion, new data cannot be used by an estimation procedure between times k and $k + \phi_k$. In a real system, a real-time state estimate must always be available for effective monitoring. We assume that two parallel jobs are executed. A support

subroutine processes received measurements and computes a state estimate at time k in ϕ_k time (cf. Fig. 2). The real-time estimation routine computes one-step-ahead open-loop updates at each point in time according to the nominal dynamics (1) (progressively degrading estimation quality), and resets when the support subroutine outputs an updated estimate with new measurements (with higher estimate quality).² A schematic representation is shown in Fig. 3. Importantly, degradation of estimation in the top plot is not due to lack of new measurements (like in Age of Information literature), but is caused by constrained resources that induce a computational bottleneck in the support subroutine (bottom plot in Fig. 3).

B. Problem Statement

The trade-offs introduced in the previous section call for a challenging sensing design at the network level. In particular, all possible choices of local sensor processing (we address a specific choice for all sensors as a *sensing configuration*) affects global performance in a complex manner, whereby it is unclear which sensors should transmit raw measurements, with poor accuracy and possibly long communication delays, and which should refine their samples locally to produce high-quality measurements. In fact, the authors in [56] show that the optimal configuration when considering steady-state performance is nontrivial. Also, the optimal sensing configuration is time varying, in general. Thus, sensing policies $\pi_i, i \in \mathcal{V}$, have to be suitably designed to maximize the overall network performance.

The state x_k is estimated via Kalman predictor, which is the optimal state observer for linear systems driven by Gaussian noise. It can be readily shown, e.g., via state augmentation, that the Kalman predictor is optimal even with delayed or dropped measurements, whereby it suffices to ignore updates associated with missing data. Out-of-sequence arrivals can be handled by recomputing all predictor steps since the latest arrived measurement has been acquired, or by more sophisticated techniques [69], [70].

Let $\tilde{x}_k \doteq x_k - \hat{x}_k$ the estimation error of Kalman predictor at time k , and let $P_k \doteq \text{Var}(\tilde{x}_k)$ its covariance matrix. We formulate the sensing design as an optimal estimation problem.

Problem 1 (Sensing Design for Processing Network). Given system (1)–(2) and Assumptions 1–4, find the optimal sensing policies $\pi_i, i \in \mathcal{V}$, that minimize the time-averaged estimation error variance with horizon K ,

$$\arg \min_{\pi_i \in \Pi_i, i \in \mathcal{V}} \frac{1}{K} \sum_{k=k_0}^K \text{Tr}(P_k^\pi) \quad (6a)$$

$$\text{s.t.} \quad P_k^\pi = f_{\text{Kalman}}(\mathcal{Y}_k^\pi), \quad (6b)$$

$$P_{k_0}^\pi = P_0, \quad (6c)$$

where the Kalman predictor $f_{\text{Kalman}}(\cdot)$ computes at time k the state estimate \hat{x}_k^π and the error covariance matrix P_k^π using data \mathcal{Y}_k^π available at the base station according to $\pi \doteq \{\pi_i\}_{i \in \mathcal{V}}$, and Π_i gathers all causal sensing policies of the i th sensor.

Remark 3 (Difference with standard sensor selection). Sleep mode actually implements an online sensor selection. We

identify two key elements that make our framework fundamentally different from standard sensor selection in the literature. First, similarly to [56], the use of both "active" modes (raw or processing) and sleep mode targets *optimal performance*, whereas classically sensors are selected to meet budget constraints under the conventional wisdom that the more are selected, the better performance. In contrast, as discussed above, selection emerges *naturally* in our framework as a need to maximize performance, in view of the computational bottleneck at the base station that may increase the objective cost in (6). Moreover, rather than a *static, a priori* selection, we allow for *dynamical switching* to and from sleep mode, which enables performance improvement through a richer design.

III. SENSING POLICY: A CENTRALIZED IMPLEMENTATION

Problem 1 is combinatorial and raises a computational challenge in finding efficient sensing policies, because the search space may easily explode. In fact, the total number of sensing configurations does not scale with the amount of sensors, e.g., 10 sensors yield $2^{10} = 1024$ possible sensing configurations at each sampling instant. Also, Problem 1 requires to design the policy for each sensor, which is a combinatorial problem by itself that scales exponentially with the time horizon K . To further complicate things, a sensing policy π_i not only affects delay and accuracy of the i th sensor, but also determines its sampling sequence \mathcal{K}_i (cf. (3)–(4)), augmenting the search space to all possible sequences.

To partially ease the intractability of the problem, and motivated by practical applications, we restrict the domain of potential policies to reduce problem complexity while still enabling useful insights. First, we look at the simple but relevant scenario with a homogeneous network and motivate the design of a centralized policy in Section III-A. We then go back to the general scenario with a heterogeneous network and formulate a simplified version of Problem 1 in Section III-B.

Remark 4 (Complexity with multiple processing modes). In the general case where the i th sensor has C_i processing modes, there are $\prod_{i \in \mathcal{V}} (C_i + 2)$ sensing configurations in total.

A. Homogeneous Network

Sensor Model. In this scenario, all smart sensors have equal measurement noise distributions,

$$y_k^{(i)} = x_k + v_k^{(i)}, \quad v_k^{(i)} \sim \mathcal{N}(0, V_k), \quad (7)$$

with $V_k = V_{\text{raw}}$ or $V_k = V_{\text{proc}}$ for raw and processed data, respectively. Also, all sensors feature identical computational and transmission resources, given by delays $\tau_{\text{raw}}, \delta_{\text{raw}}$ for raw measurements and $\tau_{\text{proc}}, \delta_{\text{proc}}$ for processed measurements, respectively (δ in case of no compression). This *homogeneous network* models the special but relevant case where sensors are interchangeable. This happens for example with sensor networks measuring temperature in plants or chemical concentrations in reactors. Also, this model captures smart sensors collecting high-level environmental information, such as UAVs tracking the position of a body moving in space.

Centralized Policy. In this case, it is sufficient to decide *how many*, rather than *which*, sensors follow a certain mode.

²We assume that one-step-ahead open-loop steps are computationally cheap.

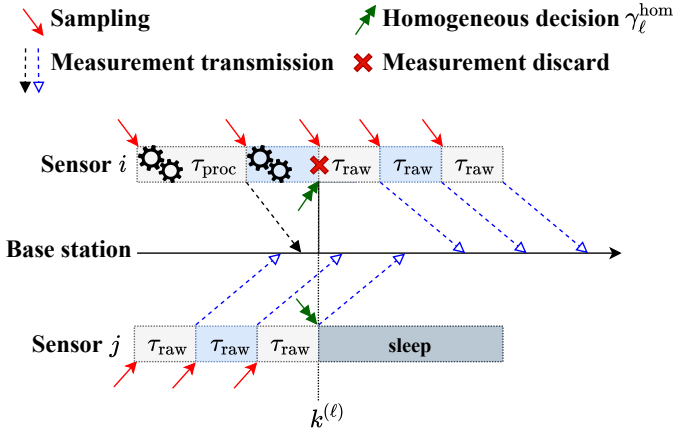


Fig. 4. **Homogeneous sensing policy.** Sampling and data processing at identical sensors are ruled by policy π_{hom} . Decision $\gamma_{\ell}^{\text{hom}}$ is communicated at time $k^{(\ell)}$ and realized at individual sensors as $\gamma_{\ell}^i = r$ and $\gamma_{\ell}^j = s$. Concurrently, the i th sensor disregards its current processed measurement (red cross) and switches to raw mode, acquiring a new sample at time $k^{(\ell)}$.

Accordingly, we focus on the design of a centralized policy that commands all sensors with no distinctions among them.

Definition 2 (Homogeneous sensing policy). A *homogeneous sensing policy* is a sequence of categorical decisions $\pi_{\text{hom}} = \{\gamma_{\ell}^{\text{hom}}\}_{\ell=1}^L$. Each decision $\gamma_{\ell}^{\text{hom}} = (N - n_s, n_p)$ is taken at time $k^{(\ell)}$ such that n_s sensors are in sleep mode and n_p out of the other $N - n_s$ sensors are in processing mode between times $k^{(\ell)}$ and $k^{(\ell+1)}$, with $0 \leq n_s \leq N$ and $0 \leq n_p \leq N - n_s$. Without loss of generality, we set $k^{(1)} = k_0$, $k^{(L)} \leq K$.

In words, the base station decides a configurations for all sensors at predefined time instants, which is both practical for applications and convenient to reduce complexity of the problem. However, decisions may be taken at any times, as long as these are consistent with sensor computational delays (e.g., to guarantee that one sample is collected for each decision).

With a slight abuse of notation, to address the mode of a specific sensor that is following the homogeneous decision $\gamma_{\ell}^{\text{hom}}$, we write $\gamma_{\ell}^i = m \in \{r, p, s\}$ meaning that the i th sensor is in raw, processing, or sleep mode, respectively. We stress that in this context γ_{ℓ}^i does not represent a decision of a *single-sensor* sensing policy π_i (see Definition 1), but all decisions are centralized and γ_{ℓ}^i denotes the mode that *the base station commands* the i th sensor to obey through decision $\gamma_{\ell}^{\text{hom}}$.

Centralized decisions are communicated regardless of current sensing status. Following common practice in real-time control [71], [72], [73], [74], [75], we assume what follows.

Assumption 5 (Sampling frequency with homogeneous sensing policy). Decision $\gamma_{\ell}^{\text{hom}}$ switches mode of the minimum amount of sensors possible. If the i th sensor switches mode, the measurement currently being acquired or processed (if any) is immediately discarded. If the new commanded mode is either raw or processing, a new sample is acquired according to such new mode right after the decision $\gamma_{\ell}^{\text{hom}}$ is communicated.

Formally, given measurement $y_k^{(i)}$ sampled at time $k < k^{(\ell)}$

obeying decision $\gamma_{\ell-1}^{\text{hom}}$, the sampling dynamics (3b) becomes

$$s_i^{\text{hom}}(k) \doteq \begin{cases} k' & \text{if } k^{(\ell)} \geq k' \\ k^{(\ell)} & \text{otherwise,} \end{cases} \quad (8a)$$

$$\bar{\ell} \doteq \min_{\ell' \in \{1, \dots, L\}} \{\ell' : \ell' \geq \ell \wedge \gamma_{\ell'}^i \neq s\}. \quad (8b)$$

Further, $y_k^{(i)}$ is discarded (not transmitted) if $s_i^{\text{hom}}(k) \neq k'$.

The new sampling mechanism is depicted in Fig. 4. According to Assumption 5, a measurement is not transmitted to the base station if it is not ready when a concurrent decision is communicated. In Fig. 4 the i th sensor discards a measurement whose processing is not completed at time $k^{(\ell)}$, when a new decision switches its mode. Formally, a sensor disregards raw (resp. processed) measurements sampled at time $\bar{k} < k^{(\ell)}$ such that $\bar{k} + \tau_{\text{raw}} > k^{(\ell)}$ ($\bar{k} + \tau_{\text{proc}} > k^{(\ell)}$), i.e., their acquisition ends after a *different* mode is imposed by decision $\gamma_{\ell}^{\text{hom}}$ (cf. (8a)). We denote by $\mathcal{Y}_k^{\pi_{\text{hom}}}$ all available data at the base station at time k according to (8) and such discard mechanism imposed by policy π_{hom} , that excludes some data included in \mathcal{Y}_k (cf. (5)).

B. Heterogeneous Network

We now return to the original model (2) with heterogeneous sensors. Without loss of generality, we assume that the sensor set \mathcal{V} is partitioned into M subsets $\mathcal{V}_1, \dots, \mathcal{V}_M$, where subset \mathcal{V}_m , $m \in \{1, \dots, M\}$, is composed of homogeneous sensors of the m th class. From what discussed in the previous section, it is sufficient to specify how many sensors follow a certain mode within each subset \mathcal{V}_m . Hence, we narrow down the domain of all possible policies according to the next definition.

Definition 3 (Network sensing policy). A *network sensing policy* is a collection $\pi_{\text{net}} \doteq \{\pi_{\text{hom}, m}\}_{m=1}^M$, where each homogeneous sensing policy $\pi_{\text{hom}, m}$ is associated with homogeneous sensor subset \mathcal{V}_m , and all homogeneous decisions $\{\gamma_{\ell}^{\text{hom}, m}\}_{m=1}^M$ are communicated together at time $k^{(\ell)}$.

In Definition 3, decision times are fixed like in the homogeneous case, so that decisions are communicated to all sensors at once. At time $k^{(\ell)}$, homogeneous decision $\gamma_{\ell}^{\text{hom}, m}$ involves sensors in \mathcal{V}_m , and the overall sensing configuration is given by the ensemble of such decisions. All data available at the base station at time k are collected in $\mathcal{Y}_k^{\pi_{\text{net}}} \doteq \{\mathcal{Y}_k^{\pi_{\text{hom}, m}}\}_{m=1}^M$.

Finally, we get the following simplified problem formulation.

Problem 2 (Centralized Sensing Design for Processing Network). Given system (1)–(2) with Assumptions 1–5, find the optimal network sensing policy π_{net} that minimizes the time-averaged estimation error variance with horizon K ,

$$\arg \min_{\pi_{\text{net}} \in \Pi_{\text{net}}} \frac{1}{K} \sum_{k=k_0}^K \text{Tr}(P_k^{\pi_{\text{net}}}) \quad (9a)$$

$$\text{s.t.} \quad P_k^{\pi_{\text{net}}} = f_{\text{Kalman}}(\mathcal{Y}_k^{\pi_{\text{net}}}), \quad (9b)$$

$$P_{k_0}^{\pi_{\text{net}}} = P_0, \quad (9c)$$

where the Kalman predictor $f_{\text{Kalman}}(\cdot)$ computes at time k the state estimate $\hat{x}_k^{\pi_{\text{net}}}$ and the error covariance matrix $P_k^{\pi_{\text{net}}}$, using data available at the base station according to π_{net} , and Π_{net} is the space of causal network sensing policies.

IV. REINFORCEMENT LEARNING FRAMEWORK

By assuming complete knowledge of delays and measurement noise covariances affecting sensors in the different modes, both Problem 1 and 2 can be analytically solved. However, the computation of the exact minimizer requires to keep track of all starts and stops of data transmissions for each sensor, resulting in a cumbersome procedure which admits no closed-form expression, and requires to solve a combinatorial problem which does not scale with the number of sensors.

Moreover, the assumptions considered in the formulation of the problem may be too conservative in real-life scenarios, and the latter method does not allow for relaxations. Indeed, as long as either delays or covariances are not explicitly known or have some variability, *i.e.*, they can be modeled by proper random variables, the minimization becomes intractable. This is true even if the expectations of these random variables are known, since the dynamics in Problem 2 leads to a nonlinear behavior for the quantity to be minimized.

Hence, the problem of choosing the optimal sensing policy in order to minimize the uncertainty of estimation is tackled through a Reinforcement Learning algorithm, which allows to flexibly address the general formulation of the problem.

A. General Scenario

The Reinforcement Learning framework [76] consists of an agent interacting with an environment without having any prior knowledge of how the latter works and how its actions may impact on it. By collecting results of the interactions, which are expressed through a reward signal, the agent will learn to maximize this user-defined quantity, under the action of the unknown environment. This can be formalized with the help of the Markov Decision Process framework, in which the tuple $\langle \mathcal{S}, \mathcal{A}, \mathcal{P}, r, \gamma \rangle$ characterize all needed elements, *i.e.*, the state space \mathcal{S} ; the set of all possible actions \mathcal{A} ; the transition probabilities \mathcal{P} regulating the underlying system, which may also be deterministic; the reward function r , which is assumed to be a function of the state and the action; and the discount factor γ , weighting future rewards. The agent selects actions to be performed on the environment through a *control policy*, which is here assumed to be a deterministic function π mapping states to actions, $\pi : \mathcal{S} \rightarrow \mathcal{A}$. The goal of the learning procedure would be to identify an optimal policy $\pi^*(\cdot)$, *i.e.*, a map allowing to achieve the highest possible return G over the long run, according to the unknown transitions imposed by the environment. The return is simply defined as the expectation of the sum of rewards in an episode of K steps, *i.e.*, $G = \mathbb{E} \left[\sum_{k=1}^K r_k \right]$.

The general problem can then be written as

$$\max_{\pi \in \Pi} \mathbb{E}_{\pi} \left[\sum_{k=0}^{K-1} \gamma^k r(s_k, a_k) \right] \quad (10a)$$

$$\text{s.t.} \quad s_{k+1}^{\pi} = g(s_k, a_k) = g(s_k, \pi(s_k)) \doteq g_{\pi}(s_k), \quad (10b)$$

for a generic state-transition function $g : \mathcal{S} \times \mathcal{A} \rightarrow \mathcal{S}$ representing environment dynamics that embeds the transition probabilities \mathcal{P} . One of the simplest and most popular

approaches to solve the maximization in (10) is the Q-learning algorithm [77].

Q-learning is a *model-free* algorithm which finds an optimal policy to maximize the expected value of the return, without learning an explicit model of the environment. This is done by focusing solely on the *values* of actions at different states, which correspond to the return.

In the tabular setting this method actually builds a lookup table with the action-value for each state-action pair, and updates it with an *optimistic* variant of the temporal-difference error [78] at every step, weighted by a learning rate α .

The action-value function is defined as

$$Q^{\pi}(s, a) = \mathbb{E}_{\pi} \left[\sum_{k=0}^{K-1} \gamma^k r(s_k, a_k) \middle| s_k = s, a_k = a \right], \quad (11)$$

and it expresses the expected return obtained by performing action a at state s and then following policy π afterwards.

The Q-learning algorithm iteratively updates an estimate of the action-value function \hat{Q} , replacing the current estimate with the one given by the best performing action and bootstrapping for the future predictions.

By defining the optimistic variant of the temporal-difference error as

$$\zeta_k^{\pi}(s, a) = r(s, a) + \gamma \max_{a'} [\hat{Q}_k(s', a')] - \hat{Q}_k(s, a), \quad (12)$$

the update for the Q-learning algorithm is given by

$$\hat{Q}_{k+1}(s, a) = \begin{cases} \hat{Q}_k(s, a) + \alpha \zeta_k^{\pi}(s, a) & \text{if } k < K - 1, \\ (1 - \alpha) \hat{Q}_k(s, a) + \alpha r(s_k, a_k) & \text{otherwise.} \end{cases} \quad (13)$$

The Q-function is updated at each step $k = 1, 2, \dots$ of one episode. The policy deployed in the environment to run the episodes and collect rewards (*behavioral policy*) is usually chosen as the ϵ -greedy policy according to the current lookup table, emphasizing the explorative behavior of the algorithm.

In a finite MDP, this approach is known to converge to the *optimal* action-value function under the standard Monro-Robbins conditions [79].

B. Optimizing Latency-Accuracy Trade-off

With regard to Problem 1, policy π_i is composed of categorical variables corresponding to sensing modes, and characterizes the potential for intervention in the operations of the i th sensor. The constraints due to the centralized implementation in Problem 2 allow us to consider a simplified policy $\pi_{\text{net}} : \mathcal{S} \rightarrow \mathcal{A}$ describing how many sensors are required to process or sleep. Specifically, each action $a \in \mathcal{A}$ is specified by pairs of integers (cf. Definition 2) dictating the amount of sensors that send data and process their measurements within each group \mathcal{V}_m after a is applied. For example, if $\mathcal{V} = \mathcal{V}_1 \cup \mathcal{V}_2$ with $|\mathcal{V}_1| = 4$ and $|\mathcal{V}_2| = 5$, action $a = \{(2, 1), (3, 0)\}$ means that two sensors transmit, with one in processing mode, and the other two sleep within \mathcal{V}_1 , and similarly for \mathcal{V}_2 .

Since we aim to minimize the time-averaged error variance (9a), a straightforward metric to be chosen as reward function is the negative trace of matrix $P_k^{\pi_{\text{net}}}$, which evolves according to the Kalman predictor with delayed updates

(Appendix A). In the considered framework the base station is allowed to change sensing configuration (corresponding to a new action) at each time $k^{(\ell)}$, therefore a natural way of defining the reward is to take the average of the negative trace of the covariance during the interval between times $k^{(\ell)}$ and $k^{(\ell+1)}$, so that the base station can appreciate the performance of a particular sensing configuration in that interval.

This leads to the following instantiation of maximization (10),

$$\max_{\pi_{\text{net}} \in \Pi_{\text{net}}} - \mathbb{E} \left[\sum_{\ell=1}^L \frac{\gamma^\ell}{k^{(\ell+1)} - k^{(\ell)}} \sum_{k=k^{(\ell)}}^{k^{(\ell+1)}} \text{Tr} (P_k^{\pi_{\text{net}}}) \right] \quad (14a)$$

$$\text{s.t.} \quad P_k^{\pi_{\text{net}}} = f_{\text{Kalman}} (\mathcal{Y}_k^\pi), \quad (14b)$$

$$P_{k_0}^{\pi_{\text{net}}} = P_0, \quad (14c)$$

with $k^{(L+1)} \doteq K$. The quantity of interest is the trace of the error covariance and thus a straightforward approach would suggest to take $\mathcal{S} = \mathbb{R}^+$, however to keep the Q-learning in a tabular setting the state space has been discretized through the function $\mathfrak{d} : \mathbb{R}^+ \rightarrow \mathbb{N}^+$. In particular, the image of $\mathfrak{d}[\cdot]$ is given by M bins, which were manually tuned in our numerical experiments to yield a fair representation of the values of $P_k^{\pi_{\text{net}}}$ observed along the episodes. Then, based on the bin associated with $\text{Tr} (P_{k^{(\ell)}})$, the agent outputs a sensing configuration $a \in \mathcal{A}$ through $\pi_{\text{thom}}(\cdot)$ at each time $k^{(\ell)}$, given by $a_\ell = \pi_{\text{thom}} \left(\mathfrak{d} \left[\text{Tr} (P_{k^{(\ell)}}) \right] \right)$.

Also, choosing $\gamma = 1$ and time intervals $[k^{(\ell)}, k^{(\ell+1)}]$ of equal length allows (14) to match objective cost (9a) exactly.

Remark 5 (Multi-agent learning). Another way to tackle Problem 1 is resorting to distributed learning schemes such as multi-agent Reinforcement Learning. However, this approach requires a dedicated design and it is left for future work. Conversely, here we build on ideas introduced in [56] to explore how the latency-accuracy trade-off impacts performance and the role of learning-based techniques in improving the sensing design.

V. NUMERICAL SIMULATIONS RESULTS

We validate performance of our proposed approach against baseline design choices with two experiments.³

In Section V-A, we consider smart sensors monitoring an autonomous vehicle to get insight into allocation of processing. In Section V-B, we address drones for target tracking and see how online sensor selection helps improve performance. Finally, in Section V-C we discuss about the role of Reinforcement Learning in conjunction with Kalman predictor, arguing in favor of a hybrid algorithmic-learning estimation framework.

A. Smart Sensing for Self-Driving Vehicle

For the first scenario, we addressed a self-driving car traveling at approximately constant speed. Specifically, we considered its transversal position with respect to the center of the lane, measured by sensors that transmit to a microcontroller (base station), which orchestrates communication and tracks the car trajectory (Fig. 5). The car position was modeled with (1)

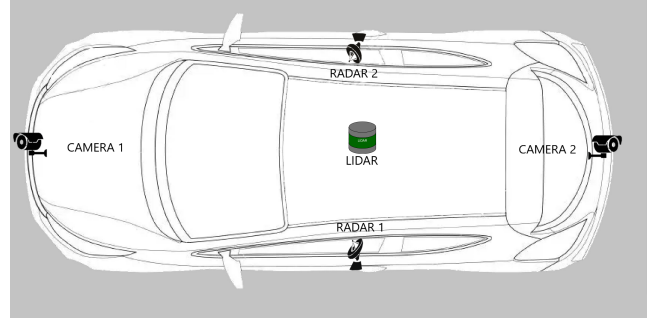


Fig. 5. Simulation setup for autonomous-driving scenario: sensors measure the car position, and a centralized microcontroller tracks its trajectory.

TABLE I
SENSOR PARAMETERS FOR AUTONOMOUS DRIVING SCENARIO.

| | Freq. | τ_{raw} | τ_{proc} | v_{raw} | v_{proc} |
|--------|-------|---------------------|----------------------|------------------|-------------------|
| Radar | 50Hz | 20ms | 30ms | 0.45 | 0.40 |
| Camera | 25Hz | 40ms | 100ms | 0.3 | 0.05 |
| Lidar | 10Hz | 100ms | 110ms | 0.09 | 0.054 |

as a double integrator, which is a flexible choice used for uncertain dynamic with direct control of accelerations [46], [80], [81], [82], [83]. This example mimics a lane shift at sustained speed (e.g., for passing or on a highway). Given such model, Kalman predictor arguably is an effective and robust estimator, assuming that lateral movements are limited compared to the car speed.

We simulated two radar devices, two cameras and one lidar, which are commonly employed in self-driving applications [84]. Many techniques used in autonomous driving exploit lidar point clouds, such as segmentation, detection and classification tasks [85]. Also, radars are emerging as a key technology for such systems. Some of today's self-driving cars, e.g., Zoox, are equipped with more than 10 radars providing 360° surrounding sensing capability under any weather conditions [86]. Finally, camera images are essential to enable commercialization of self-driving cars with autonomy at level 3 [87]. The sensor parameters (Table I, with $v_{\text{raw}}I$ and $V_{\text{proc}} = v_{\text{proc}}I$) were chosen based on real-world experiments [88], with sampling period $T = 1\text{ms}$ to ensure real-time vehicle control.

The communication protocol was simulated through the discrete-event simulator Objective Modular Network Testbed in C++ (OMNeT++) [89]. OMNeT++ is widely adopted to simulate wireless networks, because it combines standard communication protocols (e.g., IEEE 802.11) and the possibility to create customized procedures exploiting existing modules. Further, it enables realistic simulations by accurately modeling

TABLE II
LEARNING HYPERPARAMETERS FOR AUTONOMOUS-DRIVING SCENARIO.












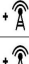
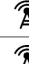
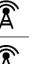

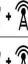

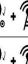

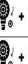







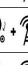


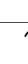



















| M | α | ϵ_0 | ϵ_{\min} | ϵ_t | γ |
|-----|----------|--------------|-------------------|--|----------|
| 5 | 0.1 | 0.2 | 0.01 | $\max \left\{ \frac{\epsilon_0}{\sqrt{t+1}}, \epsilon_{\min} \right\}$ | 1 |

³Code available at <https://github.com/lucaballotta/ProcessingNetworks-RL>.

both the electromagnetic environment and the lower layers of the protocol stack (from physical to transportation layers). In our simulations, sensors carry IEEE 802.11 (so-called Wi-Fi) communication boards.

As for training, we set five time windows each with duration 300ms. The training phase lasted 100000 episodes with hyperparameters in Table II, where t means the t th episode.

TABLE III
LEARNED NETWORK SENSING POLICY FOR AUTONOMOUS-DRIVING SCENARIO.

| | 1 | 2 | 1 | 2 | 1 |
|------------------------------|---|---|---|---|---|
| $\text{Tr}(P) > 4.25$ |  +  |  +  |  +  |  +  |  +  |
| $3.64 < \text{Tr}(P) < 4.25$ |  +  |  +  |  +  |  +  |  +  |
| $3.36 < \text{Tr}(P) < 3.64$ |  +  |  +  |  +  |  +  |  +  |
| $3.18 < \text{Tr}(P) < 3.36$ |  +  |  +  |  +  |  +  |  +  |
| $\text{Tr}(P) < 3.18$ |  +  |  +  |  +  |  +  |  +  |

From Table III we can infer that the learned policy requires processing almost from all the sensors when the error variance is high (top row). However, the need for processing diminishes with the variance, turning to raw mode both lidar and radars at the smallest values (bottom row). Interestingly, processing mode is always chosen for cameras, revealing that refining of image frames overhangs the additional computational delay. Note that in this case, given the small amount of sensors, the fusion delays induced at the base station are negligible and sleep mode is never selected, namely, sensors always transmit.

The learned policy was tested against two standard design choices: all sensors send raw measurements (*all-raw*), or all process (*all-processing*). The outcomes over the optimized horizon are plotted in Fig. 6 and summarized in Table IV.

As it is possible to appreciate from Fig. 6, the proposed policy (*Q-learning*) cleverly allocates computational resources according to the current estimate accuracy. During the transient phase (till 600ms), when the error variance is larger, processing mode is selected for lidar, cameras and one radar, according to the first two rows in Table III. Indeed, such choice performs very close to all-processing (red curve), while the all-raw configuration is clearly disadvantageous (higher blue curve). Conversely, at steady state only the cameras are left in

TABLE IV
MEAN ERROR VARIANCE IN AUTONOMOUS-DRIVING SIMULATION.

| Q-learning (proposed) | All-raw | All-processing |
|-----------------------|---------|----------------|
| 3.67 | 3.89 | 3.88 |

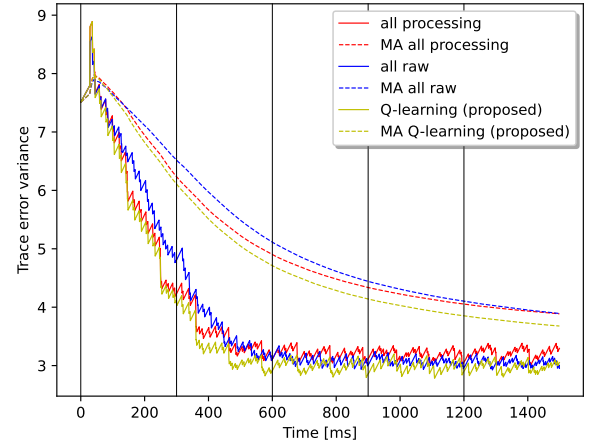


Fig. 6. Error variance in autonomous-driving simulation.

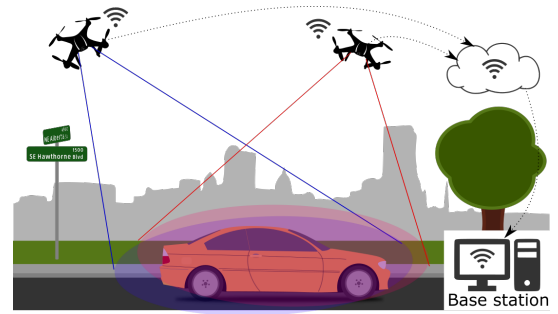


Fig. 7. Simulation setup for drone-tracking scenario: the base station monitors the target (car) trajectory based on visual updates from drones.

processing mode: this resembles more closely the all-raw policy, which performs better (lower blue curve) than all-processing.

Overall, we can see from Table IV that the proposed approach leads to a total improvement of about 6% compared to baseline policies. While this result may look marginal, we note that the improvement is rather small over the main transient phase, because the Kalman predictor is able to drop the error variance very quickly for all sensing configurations, but is way larger (about 15 – 20%) when the curves settle about small values. Also, while the objective cost (9a) refers to the whole horizon, we note that in fact the learned policy performs better than the baselines nearly at each point in time, as Fig. 6 shows, with the curve obtained with the Q-learning policy being almost always below the others. Further, the moving average (MA) is consistently smaller than both all-raw and all-processing, highlighting an even better performance of the proposed approach with respect to the targeted optimization.

Finally, we can state that, in this context, the advantage of using the proposed approach is clear: the learned policy exploits knowledge of system dynamics to select the best sensing configurations at different points in time, while baselines cannot adapt to transient and steady-state regimes, which are optimized by different processing configurations.

B. Team of Drones for Target Tracking

For our second simulation, we considered a team of 25 drones tracking a vehicle on the road (Fig. 7), modeled as a

TABLE V
SENSOR PARAMETERS FOR DRONE-TRACKING SCENARIO.

| T | τ_{raw} | τ_{proc} | v_{raw} | v_{proc} |
|------|---------------------|----------------------|------------------|-------------------|
| 10ms | 40ms | 140ms | 10 | 1 |

TABLE VI
LEARNING HYPERPARAMETERS FOR DRONE-TRACKING SCENARIO.

| M | α | ϵ_0 | ϵ_{\min} | ϵ_t | γ |
|-----|----------|--------------|-------------------|--|----------|
| 5 | 0.002 | 0.9 | 0.1 | $\max \left\{ \frac{\epsilon_0}{\sqrt{t+1}}, \epsilon_{\min} \right\}$ | 1 |

double integrator akin [56]. Each drone is equipped with a smart camera and can either transmit raw images or perform neural object detection on-board, and send fairly precise bounding boxes. The used parameters (Table V) are based on experiments in [90], [91]. In this case, given practical limitations of handling many network nodes in OMNeT++, we simulated the scenario using Python scripts and setting communication delays $\delta = 10\text{ms}$. Also, we set the fusion delay ϕ_k to be proportional to the number of data that are processed by Kalman predictor to compute \hat{x}_k . Finally, we addressed an optimization horizon with ten 500ms-long windows and Q-learning hyperparameters reported in Table VI.

The comparison between our proposed approach and baselines is shown in Fig. 8 and Table VII. In this case, performing an online selection through the sleep mode improves overall performance: in detail, 10 drones are active in raw mode during the transient (first window) and 20 through the rest of the horizon. This means that, with this setup, edge data processing is not convenient through resource constraints at drones that cause overlong computational delays. In addition,

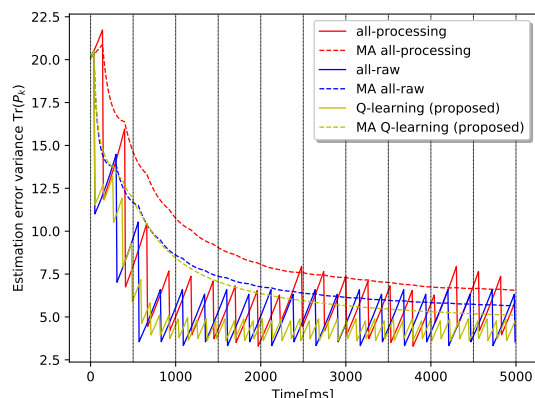


Fig. 8. Error variance in drone-based tracking simulation.

TABLE VII
MEAN ERROR VARIANCE IN DRONE-TRACKING SIMULATION.

| Q-learning (proposed) | All-raw | All-processing |
|-----------------------|---------|----------------|
| 5.10 | 5.69 | 6.58 |

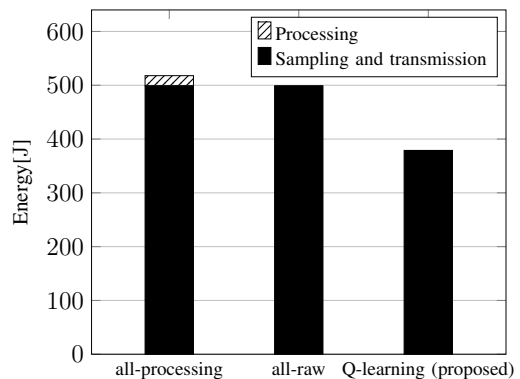


Fig. 9. Total energy consumption in drone-tracking simulation.

TABLE VIII
ENERGY CONSUMPTION BREAKDOWN DURING TRANSIENT (TRANS.) AND AT STEADY STATE (SS.) IN DRONE-TRACKING SIMULATION.

| | Q-learning (proposed) | | All-raw | | All-processing | |
|--------|-----------------------|-------|---------|-------|----------------|-------|
| | Tx | Proc. | Tx | Proc. | Tx | Proc. |
| Trans. | 59.6J | 0 | 99.8J | 0 | 99.8J | 3.8J |
| Ss. | 319.2J | 0 | 399.0J | 0 | 399.0J | 15.2J |
| Total | 378.8J | | 498.8J | | 517.8J | |

transmission of data from all drones deteriorates performance because of resource constraints at the base station, which cannot efficiently handle the incoming data stream and introduces extra computation latency.

Similarly to the first scenario (previous section), both baselines are outperformed by optimization (9), with an improvement of over 10% (see Table VII). Moreover, the variance MA is consistently smaller for the learned policy, with the exception of some short intervals within the first two windows (see Fig. 8). Also in this case, we observe that the largest improvement is registered at steady-state, while during the transient all curves are very close, with the all-raw configuration performing best at times. This may have two causes: the transient phase is more difficult to explore for the Q-learning, but also, that seemingly sub-optimal behavior during the first two windows might be necessary given that the learning procedure targets the whole horizon. Indeed, the optimal solution need not patch together the policies that optimize different segments of the horizon.

Remark 6 (Energy consumption). As an interesting side effect, the online selection also reduces the total energy consumption, potentially increasing the overall lifespan of the system besides enhancing performance. Considering industrial devices such as Genie Nano cameras [92], with typical power consumption of 3.99W for sampling and transmission (tx), and assuming an increase of 0.15W for data processing (proc.) [93], the energy consumption under the confronted sensing policies is shown in Fig. 9 and Table VIII. In particular, the proposed learning-based policy only uses 76% of the energy needed to acquire images and transmit them over wireless.

C. Discussion: the Role of Learning in Algorithmic Estimation

The proposed simulations show that the studied approach can improve performance of smart sensor networks dealing with estimation tasks. In particular, it is noteworthy that a learning framework such as Q-learning can effectively drive the sensing design, leading to improvement with respect to baselines, even with an estimation tool as effective and robust as the Kalman predictor. Indeed, the characteristics of such algorithm, applied to the chosen dynamical systems, are such that one can expect even trivial choices (such as all-raw and all-processing) to yield satisfactory performances. Conversely, a careful design given available options is far from trivial. In fact, even the most simple sensing design bears a combinatorial structure which makes it computationally infeasible to derive the optimal solution. Moreover, submodularity and supermodularity, which allow to analytically bound suboptimality gaps of greedy algorithms [46], may be hard to meet in realistic scenarios – for example, in the presence of delays, out-of-sequence message arrivals, or multi-rate sensors [56].

Given these premises, the performance improvements obtained via the studied learning method are encouraging not only with regard to the proposed applications, but mostly in supporting the contribution of such tools to classical estimation and control frameworks, which can benefit from the power of data to circumvent classical computational bottlenecks associated with an optimization-based design. Hence, rather than looking at the two domains of model-based and data-driven control as alternative approaches, we hope with this work to reinforce arguments supporting a unified, hybrid framework that picks the best of both worlds and combines them together.

VI. CONCLUSION

Motivated by smart sensing for Edge Computing applications, we have proposed an adaptive design that addresses impact of resource-constrained data sampling, processing, and transmission on performance of a monitoring task. Starting from a suitable mathematical framework modeling the considered class of systems, we have tackled the sensing design problem via Q-learning, showing that learning a data-driven policy can considerably improve the overall system performance, as well as outperforming common design choices and static sensing policies.

REFERENCES

- [1] H. Sun, Q. Guo, J. Qi, V. Ajjarapu, R. Bravo, J. Chow, Z. Li, R. Moghe, E. Nasr-Azadani, U. Tamrakar, G. N. Taranto, R. Tonkoski, G. Valverde, Q. Wu, and G. Yang, "Review of challenges and research opportunities for voltage control in smart grids," *IEEE Trans. Power Syst.*, vol. 34, no. 4, pp. 2790–2801, 2019.
- [2] H. Erdem and V. Gungor, "On the lifetime analysis of energy harvesting sensor nodes in smart grid environments," *Ad Hoc Networks*, vol. 75-76, pp. 98–105, 2018.
- [3] P. K. Reddy Maddikunta, S. Hakak, M. Alazab, S. Bhattacharya, T. R. Gadekallu, W. Z. Khan, and Q.-V. Pham, "Unmanned aerial vehicles in smart agriculture: Applications, requirements, and challenges," *IEEE Sensors J.*, vol. 21, no. 16, pp. 17 608–17 619, 2021.
- [4] K. Haseeb, I. Ud Din, A. Almogren, and N. Islam, "An energy efficient and secure iot-based wsn framework: An application to smart agriculture," *Sensors*, vol. 20, no. 7, 2020.
- [5] A. Bueno, M. Godinho Filho, and A. G. Frank, "Smart production planning and control in the industry 4.0 context: A systematic literature review," *Comput. Ind. Eng.*, vol. 149, p. 106774, 2020.
- [6] D. Ivanov, S. Sethi, A. Dolgui, and B. Sokolov, "A survey on control theory applications to operational systems, supply chain management, and industry 4.0," *Annu. Rev. Control*, vol. 46, pp. 134–147, 2018.
- [7] M. Krugh and L. Mears, "A complementary cyber-human systems framework for industry 4.0 cyber-physical systems," *Manuf. Lett.*, vol. 15, pp. 89–92, 2018, industry 4.0 and Smart Manufacturing.
- [8] B. Taner, R. Bhusal, and K. Subbarao, "A nested robust controller design for interconnected vehicles," in *Proc. AIAA Scitech Forum*, 2020.
- [9] V. Giammarino, S. Baldi, P. Frasca, and M. L. D. Monache, "Traffic flow on a ring with a single autonomous vehicle: An interconnected stability perspective," *IEEE Trans. Intell. Transp. Syst.*, vol. 22, no. 8, pp. 4998–5008, 2021.
- [10] P. A. Rad, D. Hofmann, S. A. Pertuz Mendez, and D. Goehringer, "Optimized deep learning object recognition for drones using embedded gpu," in *Proc. IEEE ETFA*, 2021, pp. 1–7.
- [11] S. Laso, M. Linaje, J. Garcia-Alonso, J. M. Murillo, and J. Berrocal, "Deployment of apis on android mobile devices and microcontrollers," in *Proc. IEEE PerCom Workshops*, 2020, pp. 1–3.
- [12] S. Li, L. Da Xu, and S. Zhao, "5G internet of things: A survey," *J. Ind. Inf. Integr.*, vol. 10, pp. 1–9, 2018.
- [13] N. Dal Fabbro, M. Rossi, G. Pillonetto, L. Schenato, and G. Piro, "Model-free radio map estimation in massive mimo systems via semi-parametric gaussian regression," *IEEE Wireless Commun. Lett.*, vol. 11, no. 3, pp. 473–477, 2022.
- [14] S. Yi, C. Li, and Q. Li, "A survey of fog computing: concepts, applications and issues," in *Proc. ACM Workshop Mobile Big Data*, 2015, pp. 37–42.
- [15] W. Shi, J. Cao, Q. Zhang, Y. Li, and L. Xu, "Edge computing: Vision and challenges," *IEEE Internet Things J.*, vol. 3, no. 5, pp. 637–646, 2016.
- [16] M. J. O'Grady, D. Langton, and G. M. P. O'Hare, "Edge computing: A tractable model for smart agriculture?" *Artif. Intell. Agriculture*, vol. 3, pp. 42–51, Sep. 2019.
- [17] S. Chen, H. Wen, J. Wu, W. Lei, W. Hou, W. Liu, A. Xu, and Y. Jiang, "Internet of Things Based Smart Grids Supported by Intelligent Edge Computing," *IEEE Access*, vol. 7, pp. 74 089–74 102, 2019.
- [18] H. Xing, O. Simeone, and S. Bi, "Decentralized federated learning via sgd over wireless d2d networks," in *Proc. IEEE SPAWC*, 2020, pp. 1–5.
- [19] M. M. Amiri, D. Gündüz, S. R. Kulkarni, and H. V. Poor, "Convergence of update aware device scheduling for federated learning at the wireless edge," *IEEE Trans. Wireless Commun.*, vol. 20, no. 6, pp. 3643–3658, 2021.
- [20] M. Chen, D. Gündüz, K. Huang, W. Saad, M. Bennis, A. V. Feljan, and H. V. Poor, "Distributed learning in wireless networks: Recent progress and future challenges," *IEEE J. Sel. Areas Commun.*, vol. 39, no. 12, pp. 3579–3605, 2021.
- [21] W. Fang, Y. Zhang, B. Yu, and S. Liu, "FPGA-based ORB feature extraction for real-time visual SLAM," in *Proc. ICIP*, Dec. 2017, pp. 275–278.
- [22] Y. Chang, Y. Tian, J. P. How, and L. Carlone, "Kimera-multi: a system for distributed multi-robot metric-semantic simultaneous localization and mapping," in *Proc. IEEE ICRA*, 2021, pp. 11 210–11 218.
- [23] M. Anvaripour, M. Saif, and M. Ahmadi, "A Novel Approach to Reliable Sensor Selection and Target Tracking in Sensor Networks," *IEEE Trans. Ind. Inform.*, vol. 16, no. 1, pp. 171–182, Jan. 2020.
- [24] L. Mao, L. Jackson, and B. Davies, "Effectiveness of a Novel Sensor Selection Algorithm in PEM Fuel Cell On-Line Diagnosis," *IEEE Trans. Ind. Electron.*, vol. 65, no. 9, pp. 7301–7310, Sep. 2018.
- [25] A. Brunello, A. Urgolo, F. Pittino, A. Montvay, and A. Montanari, "Virtual Sensing and Sensors Selection for Efficient Temperature Monitoring in Indoor Environments," *Sensors*, vol. 21, no. 8, p. 2728, Jan. 2021.
- [26] T. Devos, M. Kirchner, J. Croes, W. Desmet, and F. Naets, "Sensor Selection and State Estimation for Unobservable and Non-Linear System Models," *Sensors*, vol. 21, no. 22, p. 7492, Jan. 2021.
- [27] S. Schön, C. Brenner, H. Alkhatib, M. Coenen, H. Dbouk, N. Garcia-Fernandez, C. Fischer, C. Heipke, K. Lohmann, I. Neumann, U. Nguyen, J.-A. Paffenholz, T. Peters, F. Rottensteiner, J. Schachtschneider, M. Sester, L. Sun, S. Vogel, R. Voges, and B. Wagner, "Integrity and Collaboration in Dynamic Sensor Networks," *Sensors*, vol. 18, no. 7, p. 2400, Jul. 2018.
- [28] F. Li, M. C. De Oliveira, and R. E. Skelton, "Integrating Information Architecture and Control or Estimation Design," *SICE JCMSI*, vol. 1, no. 2, pp. 120–128, Mar. 2008.
- [29] E. Clark, S. L. Brunton, and J. N. Kutz, "Multi-Fidelity Sensor Selection: Greedy Algorithms to Place Cheap and Expensive Sensors With Cost Constraints," *IEEE Sensors J.*, vol. 21, no. 1, pp. 600–611, Jan. 2021.
- [30] M. Alonso, H. Amaris, D. Alcalá, and D. M. Florez R., "Smart Sensors for Smart Grid Reliability," *Sensors*, vol. 20, no. 8, p. 2187, Jan. 2020.

- [31] M. F. Khan, M. Bibi, F. Aadil, and J.-W. Lee, "Adaptive Node Clustering for Underwater Sensor Networks," *Sensors*, vol. 21, no. 13, p. 4514, Jun. 2021.
- [32] S. T. Jawaid and S. L. Smith, "Submodularity and greedy algorithms in sensor scheduling for linear dynamical systems," *Automatica*, vol. 61, pp. 282–288, Nov. 2015.
- [33] V. Gupta, T. H. Chung, B. Hassibi, and R. M. Murray, "On a stochastic sensor selection algorithm with applications in sensor scheduling and sensor coverage," *Automatica*, vol. 42, no. 2, pp. 251–260, Feb. 2006.
- [34] D. Maity, D. Hartman, and J. S. Baras, "Sensor scheduling for linear systems: A covariance tracking approach," *Automatica*, vol. 136, p. 110078, Feb. 2022.
- [35] L. Schenato, B. Sinopoli, M. Franceschetti, K. Poolla, and S. S. Sastry, "Foundations of Control and Estimation Over Lossy Networks," *Proc. IEEE*, vol. 95, no. 1, pp. 163–187, Jan. 2007.
- [36] A. Chiuso, N. Laurenti, L. Schenato, and A. Zanella, "LQG cheap control subject to packet loss and SNR limitations," in *ECC*, Jul. 2013, pp. 2374–2379.
- [37] S. Tatikonda and S. Mitter, "Control under communication constraints," *IEEE Trans. Autom. Control*, vol. 49, no. 7, pp. 1056–1068, Jul. 2004.
- [38] V. S. Borkar and S. K. Mitter, "LQG Control with Communication Constraints," in *Communications, Computation, Control, and Signal Processing: a tribute to Thomas Kailath*, A. Paulraj, V. Roychowdhury, and C. D. Schaper, Eds. Boston, MA: Springer US, 1997, pp. 365–373.
- [39] J. Le Ny and G. J. Pappas, "Differentially Private Filtering," *IEEE Trans. Autom. Control*, vol. 59, no. 2, pp. 341–354, Feb. 2014.
- [40] E. Shafieepoorfard and M. Raginsky, "Rational inattention in scalar LQG control," in *IEEE CDC*, Dec. 2013, pp. 5733–5739.
- [41] G. N. Nair and R. J. Evans, "Stabilizability of Stochastic Linear Systems with Finite Feedback Data Rates," *SIAM J. Control Optim.*, vol. 43, no. 2, pp. 413–436, Jan. 2004.
- [42] M. Pezzutto, F. Tramarin, S. Dey, and L. Schenato, "Adaptive transmission rate for LQG control over Wi-Fi: A cross-layer approach," *Automatica*, vol. 119, p. 109092, Sep. 2020.
- [43] P. Park, S. Coleri Ergen, C. Fischione, C. Lu, and K. H. Johansson, "Wireless Network Design for Control Systems: A Survey," *IEEE Commun. Surveys Tuts.*, vol. 20, no. 2, pp. 978–1013, 2018.
- [44] F. Branz, R. Antonello, M. Pezzutto, S. Vitturi, F. Tramarin, and L. Schenato, "Drive-by-Wi-Fi: Model-Based Control Over Wireless at 1 kHz," *IEEE Trans. Control Syst. Technol.*, vol. 30, no. 3, pp. 1078–1089, May 2022.
- [45] H. Li and Y. Shi, "Network-Based Predictive Control for Constrained Nonlinear Systems With Two-Channel Packet Dropouts," *IEEE Trans. Ind. Electron.*, vol. 61, no. 3, pp. 1574–1582, Mar. 2014.
- [46] V. Tzoumas, L. Carlone, G. J. Pappas, and A. Jadbabaie, "Lqg control and sensing co-design," *IEEE Trans. Autom. Control*, vol. 66, no. 4, pp. 1468–1483, 2021.
- [47] G. Zardini, A. Censi, and E. Frazzoli, "Co-design of autonomous systems: From hardware selection to control synthesis," in *Proc. ECC*, 2021, pp. 682–689.
- [48] V. Tripathi, L. Ballotta, L. Carlone, and E. Modiano, "Computation and communication co-design for real-time monitoring and control in multi-agent systems," in *Proc. WiOpt*, 2021, pp. 1–8.
- [49] J. R uth, R. Glebke, T. Ulmen, and K. Wehrle, "Demo abstract: Towards in-network processing for low-latency industrial control," in *IEEE INFOCOM WKSHPs*, Apr. 2018, pp. 1–2.
- [50] B. Lin, F. Zhu, J. Zhang, J. Chen, X. Chen, N. N. Xiong, and J. Lloret Mauri, "A Time-Driven Data Placement Strategy for a Scientific Workflow Combining Edge Computing and Cloud Computing," *IEEE Trans. Ind. Informat.*, vol. 15, no. 7, pp. 4254–4265, Jul. 2019.
- [51] T. Taami, S. Krug, and M. O'Nils, "Experimental Characterization of Latency in Distributed IoT Systems with Cloud Fog Offloading," in *IEEE WFCS*, May 2019, pp. 1–4.
- [52] Y.-H. Kao, B. Krishnamachari, M.-R. Ra, and F. Bai, "Hermes: Latency Optimal Task Assignment for Resource-constrained Mobile Computing," *IEEE Trans. Mobile Comput.*, vol. 16, no. 11, pp. 3056–3069, Nov. 2017.
- [53] X. Lyu, H. Tian, W. Ni, Y. Zhang, P. Zhang, and R. P. Liu, "Energy-Efficient Admission of Delay-Sensitive Tasks for Mobile Edge Computing," *IEEE Trans. Commun.*, vol. 66, no. 6, pp. 2603–2616, Jun. 2018.
- [54] R. D. Yates, Y. Sun, D. R. Brown, S. K. Kaul, E. Modiano, and S. Ulukus, "Age of Information: An Introduction and Survey," *IEEE J. Sel. Areas Commun.*, vol. 39, no. 5, pp. 1183–1210, May 2021.
- [55] A. Kosta, N. Pappas, A. Ephremides, and V. Angelakis, "The Cost of Delay in Status Updates and Their Value: Non-Linear Ageing," *IEEE Trans. Commun.*, vol. 68, no. 8, pp. 4905–4918, Aug. 2020.
- [56] L. Ballotta, L. Schenato, and L. Carlone, "Computation-communication trade-offs and sensor selection in real-time estimation for processing networks," *IEEE Trans. Netw. Sci. Eng.*, vol. 7, no. 4, pp. 2952–2965, 2020.
- [57] L. Ballotta, G. Peserico, and F. Zanini, "A reinforcement learning approach to sensing design in resource-constrained wireless networked control systems," in *Proc. IEEE CDC*, 2022, (to appear).
- [58] Z. Shi, W. Yao, Z. Li, L. Zeng, Y. Zhao, R. Zhang, Y. Tang, and J. Wen, "Artificial intelligence techniques for stability analysis and control in smart grids: Methodologies, applications, challenges and future directions," *Applied Energy*, vol. 278, p. 115733, Nov. 2020.
- [59] G. Baggio, D. S. Bassett, and F. Pasqualetti, "Data-driven control of complex networks," *Nat. Commun.*, vol. 12, no. 1, p. 1429, Mar. 2021, number: 1 Publisher: Nature Publishing Group.
- [60] S. Wang, T. Tuor, T. Salonidis, K. K. Leung, C. Makaya, T. He, and K. Chan, "When Edge Meets Learning: Adaptive Control for Resource-Constrained Distributed Machine Learning," in *Proc. IEEE INFOCOM*, Apr. 2018, pp. 63–71.
- [61] H. Medeiros, J. Park, and A. Kak, "Distributed Object Tracking Using a Cluster-Based Kalman Filter in Wireless Camera Networks," *IEEE J. Sel. Top. Signal Process.*, vol. 2, no. 4, pp. 448–463, Aug. 2008.
- [62] H. Yang, K. Zhang, K. Zheng, and Y. Qian, "Leveraging Linear Quadratic Regulator Cost and Energy Consumption for Ultra-reliable and Low-Latency IoT Control Systems," *IEEE Internet Things J.*, vol. 7, no. 9, pp. 8356–8371, Sep. 2020.
- [63] H. Jeon and Y. Eun, "A Stealthy Sensor Attack for Uncertain Cyber-Physical Systems," *IEEE Internet Things J.*, vol. 6, no. 4, pp. 6345–6352, Aug. 2019.
- [64] V. Radisavljevic-Gajic, S. Park, and D. Chasaki, "Vulnerabilities of Control Systems in Internet of Things Applications," *IEEE Internet Things J.*, vol. 5, no. 2, pp. 1023–1032, Apr. 2018.
- [65] S. Gros, M. Zanon, R. Quirynen, A. Bemporad, and M. Diehl, "From linear to nonlinear MPC: bridging the gap via the real-time iteration," *Int. J. Control*, vol. 93, no. 1, pp. 62–80, Jan. 2020.
- [66] M.-C. Tsai and D.-W. Gu, *Robust and Optimal Control*, ser. Advances in Industrial Control. London: Springer London, 2014.
- [67] B. Mildenhall, P. P. Srinivasan, M. Tancik, J. T. Barron, R. Ramamoorthi, and R. Ng, "Nerf: Representing scenes as neural radiance fields for view synthesis," in *Proc. ECCV*, A. Vedaldi, H. Bischof, T. Brox, and J.-M. Frahm, Eds. Cham: Springer International Publishing, 2020, pp. 405–421.
- [68] S. Zilberstein, "Using anytime algorithms in intelligent systems," *AI Magazine*, vol. 17, no. 3, p. 73, Mar. 1996.
- [69] R. Tou and J. Zhang, "Imm approach to state estimation for systems with delayed measurements," *IET Signal Process.*, vol. 10, no. 7, pp. 752–757, 2016.
- [70] A. Gopalakrishnan, N. S. Kaisare, and S. Narasimhan, "Incorporating delayed and infrequent measurements in extended kalman filter based nonlinear state estimation," *J. Process Control*, vol. 21, no. 1, pp. 119–129, 2011.
- [71] L. Greco, D. Fontanelli, and A. Bicchi, "Design and stability analysis for anytime control via stochastic scheduling," *IEEE Trans. Autom. Control*, vol. 56, no. 3, pp. 571–585, 2011.
- [72] M. Pavlidakis, S. Mavridis, N. Chrysos, and A. Bilas, "Trem: A task revocation mechanism for gpus," in *Proc. IEEE HPC/SmartCity/DSS*, 2020, pp. 273–282.
- [73] H. Lee and J. Lee, "Limited non-preemptive edf scheduling for a real-time system with symmetry multiprocessors," *Symmetry*, vol. 12, no. 1, 2020.
- [74] T. Fedullo, A. Morato, F. Tramarin, L. Rovati, and S. Vitturi, "A comprehensive review on time sensitive networks with a special focus on its applicability to industrial smart and distributed measurement systems," *Sensors*, vol. 22, no. 4, 2022.
- [75] W. Yu, M. Jia, C. Liu, and Z. Ma, "Task preemption based on petri nets," *IEEE Access*, vol. 8, pp. 11 512–11 519, 2020.
- [76] R. S. Sutton and A. G. Barto, *Reinforcement Learning: An Introduction*, 2nd ed. The MIT Press, 2018.
- [77] C. J. C. H. Watkins and P. Dayan, "Q-learning," *Mach. Learn.*, vol. 8, no. 3, pp. 279–292, May 1992.
- [78] R. S. Sutton, "Learning to predict by the methods of temporal differences," *Mach. Learn.*, vol. 3, no. 1, p. 9–44, aug 1988.
- [79] T. Jaakkola, M. Jordan, and S. Singh, "Convergence of stochastic iterative dynamic programming algorithms," in *Proc. NeurIPS*, vol. 6, 1993.
- [80] A. Barreiro, A. Baños, and E. Delgado, "Reset control of the double integrator with finite settling time and finite jerk," *Automatica*, vol. 127, p. 109536, May 2021.

- [81] H. G. Oral, E. Mallada, and D. Gayme, "On the Role of Interconnection Directionality in the Quadratic Performance of Double-Integrator Networks," *IEEE Trans. Autom. Control*, pp. 1–1, 2021.
- [82] V. Rao and D. Bernstein, "Naive control of the double integrator," *IEEE Control Syst. Magazine*, vol. 21, no. 5, pp. 86–97, Oct. 2001.
- [83] "Consensus Algorithms for Double-integrator Dynamics," in *Distributed Consensus in Multi-vehicle Cooperative Control: Theory and Applications*, ser. Communications and Control Engineering, W. Ren and R. W. Beard, Eds. London: Springer, 2008, pp. 77–104.
- [84] D. Feng, C. Haase-Schütz, L. Rosenbaum, H. Hertlein, C. Gläser, F. Timm, W. Wiesbeck, and K. Dietmayer, "Deep multi-modal object detection and semantic segmentation for autonomous driving: Datasets, methods, and challenges," *IEEE Trans. Intell. Transp. Syst.*, vol. 22, no. 3, pp. 1341–1360, 2021.
- [85] Y. Li, L. Ma, Z. Zhong, F. Liu, M. A. Chapman, D. Cao, and J. Li, "Deep learning for lidar point clouds in autonomous driving: A review," *IEEE Trans. Neural Netw. Learn. Syst.*, vol. 32, no. 8, pp. 3412–3432, 2021.
- [86] S. Sun and Y. D. Zhang, "4d automotive radar sensing for autonomous vehicles: A sparsity-oriented approach," *IEEE J. Sel. Topics Signal Process.*, vol. 15, no. 4, pp. 879–891, 2021.
- [87] B.-J. Kim and S.-B. Lee, "Safety evaluation of autonomous vehicles for a comparative study of camera image distance information and dynamic characteristics measuring equipment," *IEEE Access*, vol. 10, pp. 18 486–18 506, 2022.
- [88] S. Sun, A. P. Petropulu, and H. V. Poor, "Mimo radar for advanced driver-assistance systems and autonomous driving: Advantages and challenges," *IEEE Signal Process. Mag.*, vol. 37, no. 4, pp. 98–117, 2020.
- [89] (2020) Omnet++. ([web](#)).
- [90] A. Allan. (2019, Aug.) The big benchmarking roundup. ([web](#)).
- [91] S. Hossain and D.-j. Lee, "Deep Learning-Based Real-Time Multiple-Object Detection and Tracking from Aerial Imagery via a Flying Robot with GPU-Based Embedded Devices," *Sensors*, vol. 19, no. 15, p. 3371, Jan. 2019.
- [92] T. Dalsa. (2021) Genie nano series datasheet. ([web](#)).
- [93] M. Casares, A. Pinto, Y. Wang, and S. Velipasalar, "Power consumption and performance analysis of object tracking and event detection with wireless embedded smart cameras," in *Proc. Int. Conf. Signal Process. Commun. Syst.*, 2009, pp. 1–8.

APPENDIX

KALMAN PREDICTOR WITH DELAYED UPDATES [56]

Assume that at time $k - \phi_k$ the base station can use the following time-sorted measurements to compute \hat{x}_k ,

$$\mathcal{Y}_k = \{(y_{k_0}, V_{k_0}), \dots, (y_{k_M}, V_{k_M})\}, \quad k_i < k_{i+1}, \quad (15)$$

with $k_M \leq k - \phi_k$. The following procedure can handle out-of-sequence measurements sampled at or after time k_0 (oldest sample in (15)) and received before or at time $k - \phi_k$. For the sake of clarity, in (15) we have omitted subscripts and superscripts related to sensors. The estimation error covariance associated with \hat{x}_k given by Kalman predictor starting from P_{k_0} and using measurements in \mathcal{Y}_k is given by [56]

$$P_k = \mathcal{P}^{k_M:k} (\mathcal{U} (\dots \mathcal{U} (\mathcal{P}^{k_0:k_1} (\mathcal{U} (P_{k_0}, V_{k_0})), V_{k_1}) \dots, V_{k_M})), \quad (16)$$

where the multi-step open-loop update between time k_i and time $k_j \geq k_i$ (due to lack of measurements in (k_i, k_j)) is

$$\begin{aligned} \mathcal{P}^{k_i:k_j} (P) &= \mathcal{P}_{k_j} \circ \dots \circ \mathcal{P}_{k_i} (P), \quad \mathcal{P}^{k_i:k_i} (P) \doteq P \\ \mathcal{P}_{k_i} (P) &\doteq A_{k_i} P A_{k_i}^\top + W_{k_i}, \end{aligned} \quad (17)$$

and the update with the i th measurement sampled at time k_i is

$$\mathcal{U} (P_{k_i}, V_{k_i}) = \left((P_{k_i})^{-1} + (V_{k_i})^{-1} \right)^{-1}. \quad (18)$$